Driving and pinning forces acting on vortices in layered superconductors

M. Tachiki, S. Takahashi, and K. Sunaga
Institute for Materials Research, Tohoku University, 2-1-1 Katahira, Aoba-ku, Sendai 980, Japan
(Received 13 October 1992)

The vortex structure and the distribution of the transport current in a layered superconductor consisting of an alternate stack of strongly and weakly superconducting layers are theoretically studied within the framework of the Ginzburg-Landau theory. It is assumed that in the superconductor the coherence length is comparable to the layer thickness and the penetration depth is much longer than the thickness. The present theory predicts that the superconducting current mainly flows in the strongly superconducting layer, while the vortex center lies in the weakly superconducting layer. As a result the driving force acting on the vortex becomes extremely weak, since the small current density in the weakly superconducting layer is responsible for the force. Some behavior of the critical current in the cuprate superconductors $YBa_2Cu_3O_{7-\delta}$ and $Bi_2Sr_2CaCu_2O_{8+\delta}$ may be explained with the present theory.

I. INTRODUCTION

Experiments show that *c*-axis-oriented high-quality films of yttrium and bismuth cuprate oxides carry the large critical current density at low temperatures and the superconducting current stands up to a strong magnetic field parallel to the films.[1-9] The critical current density in bismuth cuprate oxides is independent of the relative angle between the directions of the current and the magnetic field in the film plane.[10,11] A characteristic of the films is that they have stacking structures of strongly and weakly superconducting layers. In the cuprate superconductors, the CuO_2 layers are strongly superconducting layers and the other layers are weakly superconducting layers. The experimental results mentioned above suggest that the vortices are strongly prevented from moving perpendicular to the layers in the films. We consider that this strong pinning effect originates from the nature of the layer structure itself as shown in the following way.

The vortices parallel to the layers are stable in the weakly superconducting layers. The strongly superconducting layers work as potential barriers when the vortices move perpendicular to the layers.[12-25] In addition to this pinning effect, we have the following effect to enhance the pinning. In the superconductors the transport current mainly flows in the strongly superconducting layers, and thus the current density in the weakly superconducting layers is much smaller than that in the strongly superconducting layers. In this paper we show that each vortex is driven by the transport current density just at the vortex center, even when the vortex current spreads out over many layers. Therefore, the driving force acting on the vortices in the weakly superconducting layers is very weak.

In this paper we derive the expressions for the driving force and the pinning force within the framework of the Ginzburg-Landau theory and study the nature of the vortices bound near the interface between the strongly and weakly superconducting layers. Using the theoretical results, we try to explain the experimental results of the critical current in the films of cuprate superconductors. This theory is also applicable to superconductors of artificial multilayers such as niobium/tantalum[26-28] and $YBa_2Cu_3O_{7-\delta}/PrBa_2Cu_3O_{7-\delta}$.[29-35]

II. MODEL

By the action of the driving force due to transport current in superconducting multilayers, the vortices are pinned near the interfaces between the strongly and weakly superconducting layers. To see how the vortices are pinned there, we pick up one of the interfaces and investigate the force acting on one vortex near the interface. The positions of other vortices around the vortex are fixed and their current exerts the interaction to the vortex. In other words, the other vortices are treated in a way of mean field. We assume that in the absence of the vortex under consideration, the superconducting order parameter changes stepwise at the interface as shown in Fig. 1. The quantities ψ_1 and ψ_2 are the superconducting order parameters in regions 1 and 2, respectively. If the amplitude and phase of the superconducting order parameter in the presence of the vortices are written as $\psi(\mathbf{r})$ and $\varphi(\mathbf{r})$, respectively, the Ginzburg-Landau (GL) free energy for this model is expressed as[36]

$$F=\sum_{i=1,2}\int_i d\mathbf{r}\left[\alpha_i\psi^2(\mathbf{r})+\frac{1}{2}\beta_i\psi^4(\mathbf{r})+\frac{\hbar^2}{4m_i}[\nabla\psi(\mathbf{r})]^2+\frac{\hbar^2}{4m_i}\psi^2(\mathbf{r})\left[\nabla\varphi(\mathbf{r})-\frac{2e}{\hbar c}\mathbf{A}(\mathbf{r})\right]^2+\frac{\mathbf{b}^2(\mathbf{r})}{8\pi}\right], \quad (1)$$

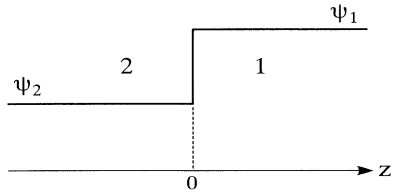

FIG. 1. Superconducting order parameter in the absence of the vortices under consideration. ψ_1 and ψ_2 denote the order parameters in regions 1 and 2, respectively.

where α_i and β_i are the GL parameters in the region i and the subscript i of the integral symbol indicates the integral over the region i. In Eq. (1), $\mathbf{A}(\mathbf{r})$ is the vector potential and $\mathbf{b}(\mathbf{r})$ is the microscopic magnetic field. Taking variation of the free energy Eq. (1) with respect to $\psi(\mathbf{r})$ and $\mathbf{A}(\mathbf{r})$, we obtain the GL equations

$$-\frac{\hbar^2}{4m_i}\nabla^2\psi(\mathbf{r})+\frac{\hbar^2}{4m_i}\psi(\mathbf{r})\left[\nabla\varphi(\mathbf{r})-\frac{2\pi}{\Phi_0}\mathbf{A}(\mathbf{r})\right]^2+\alpha_i\psi(\mathbf{r})+\beta_i\psi^3(\mathbf{r})=0\ , \tag{2}$$

$$\nabla\times\mathbf{b}(\mathbf{r})=\frac{4\pi}{c}\mathbf{j}(\mathbf{r})=-\frac{8\pi e^2\psi^2(\mathbf{r})}{m_i c^2}\left[\mathbf{A}(\mathbf{r})-\frac{\Phi_0}{2\pi}\nabla\varphi(\mathbf{r})\right]\ , \tag{3}$$

where $\mathbf{j}(\mathbf{r})$ is the superconducting current and Φ_0 is the unit flux $hc/2e$. The variation of the free energy Eq. (1) with respect to the phase $\varphi(\mathbf{r})$ gives the relation of the current conservation. We solve Eqs. (2) and (3) under the boundary conditions at the interface, which are given in Sec. V. Using the vortex solution, we study the driving and pinning forces acting on the vortex near the interface.

III. VORTEX FREE ENERGY IN THE SYSTEM

We take the x and y axes in the plane of the interface and the z axis perpendicular to the interface. A vortex that is parallel to the x axis and passes through the point ($x=0$, $y=0$, and $z=z_0$) is described by introducing a phase singularity expressed by[36]

$$\nabla\times\nabla\varphi(\mathbf{r})=2\pi\mathbf{e}_x\delta(y)\delta(z-z_0)\ , \tag{4}$$

$\mathbf{e}_x$ being the unit vector in the direction of the x axis. For simplicity, we assume that the system is homogeneous along the x axis, that is, all physical quantities are independent of x and only dependent on y and z. Hereafter, the position vector $\mathbf{r}$ stands for a two-dimensional vector (y,z) in the yz plane. The increase of the free energy due to inclusion of the vortex in the system is given from the free energy Eq. (1) with use of Eq. (3) by

$$\delta F=F_\psi+F_b\ , \tag{5}$$

with

$$F_\psi=\sum_{i=1,2}\int_i d\mathbf{r}\left[\alpha_i[\psi^2(\mathbf{r})-\psi_i^2]+\frac{\beta_i}{2}[\psi^4(\mathbf{r})-\psi_i^4]+\frac{\hbar^2}{4m_i}[\nabla\psi(\mathbf{r})]^2\right]\ , \tag{6}$$

$$F_b=\sum_{i=1,2}\int_i d\mathbf{r}\left[-\frac{1}{2c}\mathbf{j}(\mathbf{r})\cdot\left[\mathbf{A}(\mathbf{r})-\frac{\Phi_0}{2\pi}\nabla\varphi(\mathbf{r})\right]+\frac{\mathbf{b}^2(\mathbf{r})}{8\pi}\right]\ , \tag{7}$$

where ψ_i is the amplitude of the superconducting order parameter in the absence of the vortex in the region i. The free energy F_ψ is the so-called vortex core energy, which is created by the modification of the amplitude of the superconducting order parameter due to inclusion of the vortex. This local approximation is justified in the case where the distance between the vortices is much longer than the vortex core size. This free energy contributes to the pinning force.

The free energy Eq. (7) is the electromagnetic part of the free energy and is written using Eq. (3) as

$$F_b=\sum_{i=1,2}\int_i d\mathbf{r}\left[\frac{2\pi}{c^2}\lambda_i^2[\psi_i/\psi(\mathbf{r})]^2\times\mathbf{j}^2(\mathbf{r})+\frac{1}{8\pi}\mathbf{b}^2(\mathbf{r})\right]\ , \tag{8}$$

where λ_i is the penetration depth defined by

$$\lambda_i^2=m_i c^2/8\pi e^2\psi_i^2\ . \tag{9}$$

The free energy F_b contributes to both the driving force and the pinning force. Let us consider the case where an electric current is externally injected into the system in a magnetic field. In this experimental arrangement, the vortex configuration and the magnetic-field penetration from the surface and thus the microscopic superconducting current $\mathbf{j}(\mathbf{r})$ are determined in a self-consistent manner. For convenience, we divide the superconducting current into two parts[36]

$$\mathbf{j}(\mathbf{r})=\mathbf{j}_v(\mathbf{r})+\mathbf{j}_t(\mathbf{r})\ , \tag{10}$$

where $\mathbf{j}_v(\mathbf{r})$ is the vortex current and $\mathbf{j}_t(\mathbf{r})$ is the microscopic transport current defined by $\mathbf{j}(\mathbf{r})-\mathbf{j}_v(\mathbf{r})$. As seen from the definition, the current $\mathbf{j}_t(\mathbf{r})$ originates from the current of the vortices other than the vortex under consideration and from the surface current. In a similar way we divide the magnetic field into two parts

$$\mathbf{b}(\mathbf{r})=\mathbf{b}_v(\mathbf{r})+\mathbf{b}_t(\mathbf{r})\ , \tag{11}$$

where $\mathbf{b}_v(\mathbf{r})$ is the magnetic field induced by $\mathbf{j}_v(\mathbf{r})$ and $\mathbf{b}_t(\mathbf{r})$ is the magnetic field induced by $\mathbf{j}_t(\mathbf{r})$. If we insert Eqs. (10) and (11) into Eq. (8), we have

$$F_b=F_b^d+F_b^p+F_b^t\ , \tag{12}$$

with

$$F_b^d=\sum_{i=1,2}\int_i d\mathbf{r}\left[\frac{4\pi}{c^2}\lambda_i^2[\psi_i/\psi(\mathbf{r})]^2\mathbf{j}_v(\mathbf{r})\cdot\mathbf{j}_t(\mathbf{r})+\frac{1}{4\pi}\mathbf{b}_v(\mathbf{r})\cdot\mathbf{b}_t(\mathbf{r})\right], \tag{13}$$

$$F_b^p=\sum_{i=1,2}\int_i d\mathbf{r}\left[\frac{2\pi}{c^2}\lambda_i^2[\psi_i/\psi(\mathbf{r})]^2 j_v^2(\mathbf{r})+\frac{\mathbf{b}_v^2(\mathbf{r})}{8\pi}\right], \tag{14}$$

$$F_b^t=\sum_{i=1,2}\int_i d\mathbf{r}\left[\frac{2\pi}{c^2}\lambda_i^2[\psi_i/\psi(\mathbf{r})]^2\mathbf{j}_t^2(\mathbf{r})+\frac{\mathbf{b}_t^2(\mathbf{r})}{8\pi}\right]. \tag{15}$$

The free energies F_b^d and F_b^p contribute to the driving force and the pinning force, respectively.

IV. DRIVING FORCE

The free energy Eq. (13) is rewritten by using Eq. (3) as

$$\begin{aligned}F_b^d&=\sum_{i=1,2}\int_i\frac{d\mathbf{r}}{4\pi}\left[-\frac{4\pi}{c}\mathbf{j}_t(\mathbf{r})\cdot\left[\mathbf{A}_v(\mathbf{r})-\frac{\Phi_0}{2\pi}\nabla\varphi(\mathbf{r})\right]+\mathbf{b}_v(\mathbf{r})\cdot\mathbf{b}_t(\mathbf{r})\right]\\&=\sum_{i=1,2}\int_i\frac{d\mathbf{r}}{4\pi}\left[-\nabla\times\mathbf{b}_t(\mathbf{r})\cdot\left[\mathbf{A}_v(\mathbf{r})-\frac{\Phi_0}{2\pi}\nabla\varphi(\mathbf{r})\right]+\mathbf{b}_v(\mathbf{r})\cdot\mathbf{b}_t(\mathbf{r})\right],\end{aligned} \tag{16}$$

where $\mathbf{A}_v(\mathbf{r})$ is the vector potential inducing the vortex magnetic field $\mathbf{b}_v(\mathbf{r})$. Integrating the first term in the bracket of the second line in Eq. (16) by parts, we have

$$F_b^d=\sum_{i=1,2}\int_i\frac{d\mathbf{r}}{4\pi}\left[-\mathbf{b}_t(\mathbf{r})\cdot[\nabla\times\mathbf{A}_v(\mathbf{r})-\frac{\Phi_0}{2\pi}\nabla\times\nabla\varphi(\mathbf{r})]+\mathbf{b}_v(\mathbf{r})\cdot\mathbf{b}_t(\mathbf{r})\right]. \tag{17}$$

In deriving Eq. (17) we used a boundary condition in which the interface energy vanishes. The term $-\mathbf{b}_t(\mathbf{r})\cdot\nabla\times\mathbf{A}_v(\mathbf{r})$ in Eq. (17), which comes from the interaction energy between the microscopic transport current and the vector potential of the vortex, is compensated with the magnetic-field energy expressed by the last term in Eq. (17). Using Eq. (4), we have the free energy F_b^d as

$$F_b^d=\frac{\Phi_0}{4\pi}\mathbf{b}_t(\mathbf{r}_0)\cdot\mathbf{e}_x\ , \tag{18}$$

$\mathbf{r}_0$ being the position of the vortex center $(0,z_0)$. Equation (18) indicates that the free energy F_b^d is related to the magnetic field induced by the transport current just at the vortex center. The driving force is calculated from F_b^d as

$$\mathbf{f}_d=-\nabla_{\mathbf{r}_0}F_b^d=\frac{\Phi_0}{4\pi}[\nabla_{\mathbf{r}_0}\times\mathbf{b}_t(\mathbf{r}_0)]\times\mathbf{e}_x\ , \tag{19}$$

where $\nabla_{\mathbf{r}_0}$ is the derivative operator with respect to the position of the vortex center. As proven in Appendix A, $(c/4\pi)\nabla_{\mathbf{r}_0}\times\mathbf{b}_t(\mathbf{r}_0)$ is equal to the transport current at the position $\mathbf{r}_0$ in the absence of the vortex. We write this current as $j_{t0}(\mathbf{r})$ and call it the *true* transport current, since the spatial average of the true transport current is equal to the observed transport current, as proven in Appendix B. Using the true transport current, Eq. (19) is written as

$$\mathbf{f}_d=\frac{\Phi_0}{c}\mathbf{j}_{t0}(\mathbf{r}_0)\times\mathbf{e}_x\ . \tag{20}$$

The driving force is expressed by the true transport current just at the center, although the vortex current spreads out over the lengths of the penetration depths λ_1 and λ_2, which are several thousands Å in cuprate superconductors. It is worthwhile to notice that the true transport current is different from the microscopic transport current given by $(c/4\pi)\nabla\times\mathbf{b}_t(\mathbf{r})$, which vanishes at $\mathbf{r}=\mathbf{r}_0$.

The distribution of the true transport center near the interface is determined in the following way. As shown in Appendix C, we have the boundary condition at the interface

$$\lambda_1^2[j_{t0}^y(\mathbf{r})]_1=\lambda_2^2[j_{t0}^y(\mathbf{r})]_2\ , \tag{21}$$

the subscripts 1 and 2 indicating regions 1 and 2, respectively. If we write the spatial average of $j_{t0}^y(\mathbf{r})$ near the interface in regions 1 and 2 as j_1 and j_2, respectively, the boundary condition (21) is written as

$$\lambda_1^2 j_1=\lambda_2^2 j_2\ . \tag{22}$$

Then, from Eqs. (19) and (A5), the driving force acting on the vortex in region 1 is given by

$$f_d=\frac{\Phi_0}{c}j_1\ , \tag{23}$$

and the force in region 2 is given by

$$f_d=\frac{\Phi_0}{c}j_2\ . \tag{24}$$

The calculated driving force for the ratio $\lambda_2/\lambda_1=2$ is shown as a function of the position of the vortex center in Fig. 2. As seen in Fig. 2, the driving force for the vortex

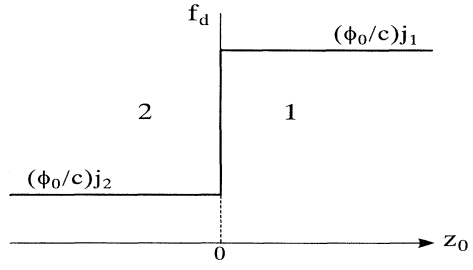

FIG. 2. Driving force f_d as a function of the vortex center z_0. j_1 and j_2 are the transport current densities in regions 1 and 2, respectively.

in region 2 is much weaker than that for the vortex in region 1, since j_2 is much smaller than j_1 as seen from the boundary condition Eq. (22).

V. PINNING FORCE

In this section we calculate the pinning forces that originate from the free energies Eqs. (6) and (14). For this purpose we should obtain $\psi(\mathbf{r})$ and $\mathbf{A}_v(\mathbf{r})$ by solving the GL equations for the vortex near the interface. The GL equations (2) and (3) are rewritten as

$$-\xi_i^2\nabla^2\psi(\mathbf{r})+\xi_i^2\left[\nabla\varphi(\mathbf{r})-\frac{2\pi}{\Phi_0}\mathbf{A}_v(\mathbf{r})\right]^2\psi(\mathbf{r}) -\psi(\mathbf{r})+\psi^3(\mathbf{r})/\psi_i^2=0 , \quad (25)$$

$$\nabla\times\nabla\times\mathbf{A}_v(\mathbf{r}) +\frac{1}{\lambda_i^2}[\psi(\mathbf{r})/\psi_i]^2\left[\mathbf{A}_v(\mathbf{r})-\frac{\Phi_0}{2\pi}\nabla\varphi(\mathbf{r})\right]=0 , \quad (26)$$

where $\xi_i=(\hbar^2/4m_i|\alpha_i|)^{1/2}$ is the coherence length of the superconductor i. The boundary conditions for $\psi(\mathbf{r})$ and $\mathbf{A}_v(\mathbf{r})$ at the interface are given in the following way.[37,38] We assume that the phase $\varphi(\mathbf{r})$ of the superconducting order parameter $\Psi(\mathbf{r})=\psi(\mathbf{r})\exp[i\varphi(\mathbf{r})]$ is continuous at the interface, and that the order parameters for both sides of the interface are related to each other with a linear relation

$$[\Psi(\mathbf{r})]_1=p[\Psi(\mathbf{r})]_2 , \quad (27)$$

where p is a constant independent of the position in the interface. In the absence of the vortex, p is given by ψ_1/ψ_2. If we assume the same value for p even in the presence of the vortex, Eq. (27) is rewritten as

$$[\psi(\mathbf{r})]_1/\psi_1=[\psi(\mathbf{r})]_2/\psi_2 . \quad (28)$$

We also assume a similar linear relation for the derivative of the order parameter in a gauge-invariant form

$$\left[\left[\nabla_z-\frac{2\pi i}{\Phi_0}A_v^z(\mathbf{r})\right]\Psi(\mathbf{r})\right]_1 =q\left[\left[\nabla_z-\frac{2\pi i}{\Phi_0}A_v^z(\mathbf{r})\right]\Psi(\mathbf{r})\right]_2 , \quad (29)$$

with a constant q. From the condition that the current

$$\mathbf{j}_v^z(\mathbf{r})=\frac{e\hbar}{2m_i i}\left[\Psi^*(\mathbf{r})\left[\nabla_z-\frac{2\pi i}{\Phi_0}A_v^z(\mathbf{r})\right]\Psi(\mathbf{r})-\text{c.c.}\right] , \quad (30)$$

is continuous at the interface, q is determined as

$$q=(m_1/m_2)(\psi_2/\psi_1) . \quad (31)$$

Using Eq. (31), from the real part of Eq. (29), we have the boundary condition

$$(\psi_1/m_1)[\nabla_z\psi(\mathbf{r})]_1=(\psi_2/m_2)[\nabla_z\psi(\mathbf{r})]_2 , \quad (32)$$

and from the imaginary part of Eq. (29) we have the boundary condition

$$\left[\frac{|\psi(\mathbf{r})|^2}{m_1}\left[A_v^z(\mathbf{r})-\frac{\Phi_0}{2\pi}\nabla_z\varphi(\mathbf{r})\right]\right]_1 =\left[\frac{|\psi(\mathbf{r})|^2}{m_2}\left[A_v^z(\mathbf{r})-\frac{\Phi_0}{2\pi}\nabla_z\varphi(\mathbf{r})\right]\right]_2 . \quad (33)$$

The condition Eq. (33) is the same as that obtained from the continuation of the current Eq. (3) at the interface. In a way similar to Appendix C, we can derive the boundary condition for the vector potential and the phase as

$$\left[A_v^y(\mathbf{r})-\frac{\Phi_0}{2\pi}\nabla_y\varphi(\mathbf{r})\right]_1=\left[A_v^y(\mathbf{r})-\frac{\Phi_0}{2\pi}\nabla_y\varphi(\mathbf{r})\right]_2 . \quad (34)$$

The amplitude of the order parameter $\psi(\mathbf{r})$ and the vector potential $\mathbf{A}_v(\mathbf{r})$ of the vortex are determined by solving the GL equations (25) and (26) under the boundary conditions Eqs. (28), (32), (33), and (34).

For $\nabla\varphi(\mathbf{r})$, we use a solution of Eq. (4),

$$\nabla\varphi(\mathbf{r})=(-z+z_0,y)/[y^2+(z-z_0)^2] . \quad (35)$$

To solve Eqs. (25) and (26) numerically, a certain domain in the yz plane, which includes the vortex and the interface, is divided into meshes. Then, we replace the differential equations (25) and (26) by difference equations with respect to the lattice points in the mesh. By solving the coupled difference equations numerically, we obtain $\psi(\mathbf{r})$ and $\mathbf{A}_v(\mathbf{r})$ for the vortex. In the numerical calculation, we assume $m_1=m_2=m$ and $\xi_2=\xi_1=\xi$, and take the parameter values of $\lambda_2/\lambda_1=2$, $\kappa_1=\lambda_1/\xi=5$, and $\kappa_2=\lambda_2/\xi=10$. The details of the numerical calculation are given in Appendix D.

A. Pinning force originating from the vortex core energy

The order parameters for the vortices at $z_0/\xi=-2$, -1, 0, 1, and 2 are, respectively, shown as functions of z/ξ in the plane of $y=0$ in Fig. 3. The solid and dotted curves indicate, respectively, the order parameters with and without the vortex in the system. The amplitude of the order parameter and its slope jump at the interface $z=0$. The loss of the order parameter due to inclusion of the vortex center in the weakly superconducting region is smaller than that in the strongly superconducting region.

Using the numerical result for $\psi(\mathbf{r})$, we calculate the pinning force originating from the vortex core energy. The free energy of the vortex core per unit length Eq. (6) is rewritten as

$$F_\psi=\sum_{i=1,2}\int_i d\mathbf{r}\frac{H_{c,i}^2}{8\pi}\left\{\left[1-\left[\frac{\psi(\mathbf{r})}{\psi_i}\right]^2\right]^2 +2\xi^2\left[\nabla\frac{\psi(\mathbf{r})}{\psi_i}\right]^2\right\} , \quad (36)$$

where $H_{c,i}=\Phi_0/(2\sqrt{2}\pi\lambda_i\xi)$ is the thermodynamic critical field of the superconductor in the region i. The quan-

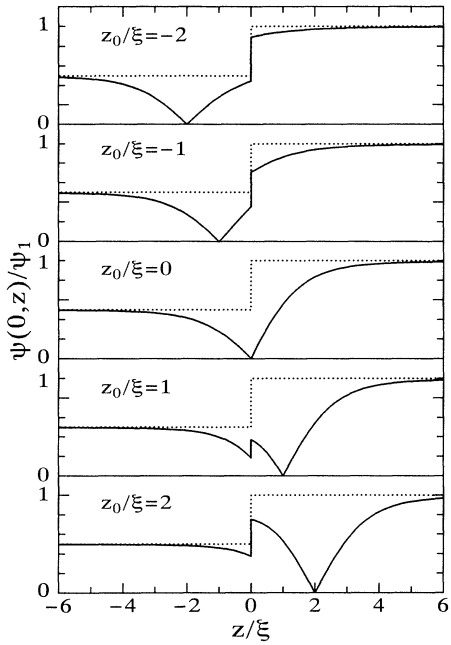

FIG. 3. Superconducting order parameters for five positions of the vortex center as functions of z/ξ in the plane of $y=0$. The solid and dotted curves indicate, respectively, the superconducting order parameters with and without the vortex in the system.

tity $H_{c,i}^2/8\pi$ in Eq. (36) is the superconducting condensation energy in the absence of the vortex. In Fig. 4, the free energy F_ψ is shown as a function of the vortex center z_0/ξ. The free energy F_ψ is normalized by

$$E=\xi^2 H_{c,1}^2/8\pi \ . \tag{37}$$

Since the vortex core radius is $\sim\xi$, the free energy drastically changes in the range $-\xi \lesssim z_0 \lesssim \xi$ around the interface.

The pinning force acting on the vortex per unit length is given by

$$f_\psi=-\frac{d}{dz_0}F_\psi \ . \tag{38}$$

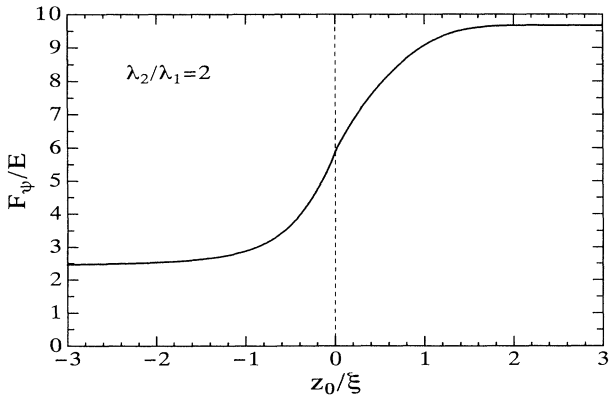

FIG. 4. Vortex core free energy F_ψ as a function of the vortex center z_0/ξ.

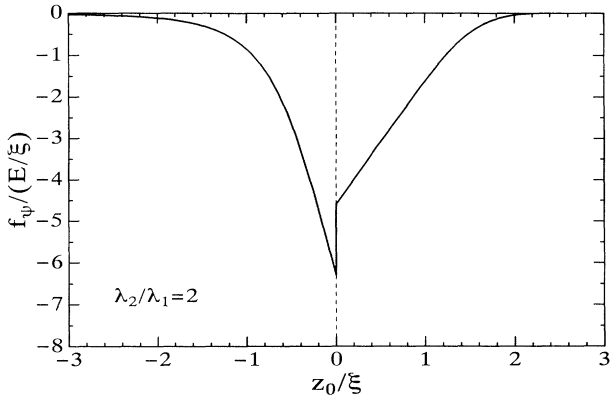

FIG. 5. Vortex core pinning force f_ψ as a function of the vortex center z_0/ξ.

Shown in Fig. 5 is the calculated pinning force as a function of the vortex center z_0/ξ. The maximum pinning force appears just at the weakly superconducting side of the interface. It is shown that the maximum pinning force rapidly increases as the ratio λ_2/λ_1 increases.

B. Pinning force originating from the electromagnetic energy of the vortex

The magnetic field $\mathbf{b}_v(\mathbf{r})$ calculated from $\nabla\times\mathbf{A}_v(\mathbf{r})$ has only the x component. The distribution of the vortex magnetic field is shown as a function of z/ξ in the plane of $y=0$ in Fig. 6. The order parameter is also shown by the dotted curves in this figure. The curves in Fig. 6 change their slope at the interface. The ratio $[db_v/dz]_1/[db_v/dz]_2$ at the interface is given by $(\lambda_2/\lambda_1)^2$ from the boundary condition Eq. (34). The magnetic field

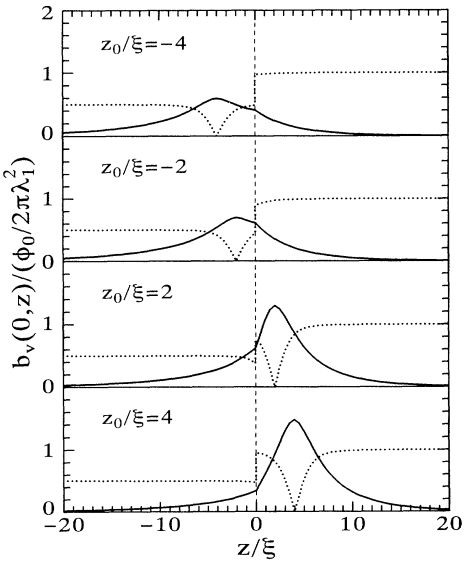

FIG. 6. Vortex magnetic fields for four positions of the vortex center as functions of z/ξ in the plane of $y=0$. The solid curves indicate the vortex magnetic fields and the dotted curves indicate the superconducting order parameters.

at the vortex center for $z_0 > 0$ is much larger than that for $z_0 < 0$.

The free energy Eq. (14) is rewritten as

$$F_b^p = \frac{\Phi_0}{8\pi} b_v(\mathbf{r}_0) - \int \frac{dS}{4\pi} \mathbf{b}_v(\mathbf{r}) \cdot \left[\left[\mathbf{A}_v(\mathbf{r}) - \frac{\Phi_0}{2\pi} \nabla\varphi(\mathbf{r}) \right]_1 \times \mathbf{e}_z - \left[\mathbf{A}_v(\mathbf{r}) - \frac{\Phi_0}{2\pi} \nabla\varphi(\mathbf{r}) \right]_2 \times \mathbf{e}_z \right] . \quad (39)$$

If the boundary condition Eq. (34) is fulfilled, Eq. (39) is reduced to

$$F_b^p = \frac{\Phi_0}{8\pi} b_v(\mathbf{r}_0) , \quad (40)$$

where $b_v(\mathbf{r}_0)$ is the vortex magnetic field at the vortex center $\mathbf{r}_0$. In Fig. 7, the free energy is shown as a function of z_0/ξ. In this figure, the core pinning energy F_ψ for $\lambda_2/\lambda_1 = 2$ is also plotted by the dotted curve for comparison.

The pinning force acting on the vortex per unit length is given by

$$f_b^p = -\frac{d}{dz_0} F_b^p = -(\Phi_0/8\pi) \frac{d}{dz_0} b_v(\mathbf{r}_0) . \quad (41)$$

The pinning force f_b^p is shown by the solid curve as a function of the vortex center z_0/ξ in Fig. 8, along with the core pinning force plotted by the dotted curve. In contrast with the core pinning force f_ψ, which shows the maximum at $z_0 = 0$, the electromagnetic pinning force f_b^p has the maximum at $z_0/\xi = 1.2$. We see that the maximum core pinning force is larger than the maximum electromagnetic pinning force. It is shown that the maximum core pinning force rapidly increases as λ_2/λ_1 increases and tends to infinity in the limit of $\lambda_2/\lambda_1 \to \infty$, while the maximum electromagnetic pinning force slightly increases and tends to a certain value. Therefore, the vortex pinning force due to the interface is dominated by the core pinning force for large values of λ_2/λ_1.

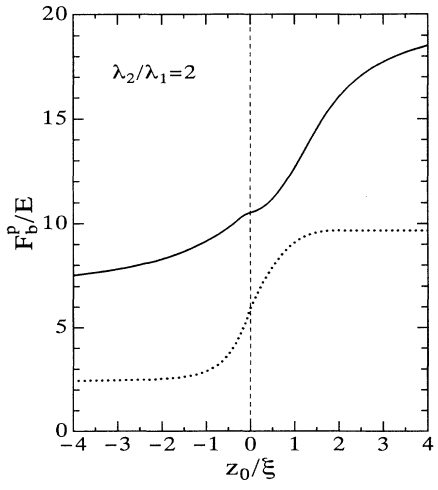

FIG. 7. Electromagnetic free energy of the vortex F_b^p is indicated as a function of the vortex center z_0/ξ by the solid curve. The vortex core energy is also plotted by the dotted curve.

In Figs. 9(a) and (b), we show the total free energy F_p, which is given by the sum of the core and electromagnetic free energies, and the total pinning force f_p, which is given by the sum of the core and electromagnetic pinning forces, respectively. As seen in Fig. 9(b), the maximum of the pinning force appears in the weakly superconducting region. This result plays a crucial role of enhancing the critical current, since the driving force is weak in this region.

VI. CRITICAL CURRENT

In this section, we demonstrate that the inhomogeneous distribution of the transport current plays an important role for the pinning of the vortex bound near the interface. Figure 10 shows the sum of the free energies Eqs. (18), (36), and (40). The curves show the free energies for the several values of the normalized transport current density in the weakly superconducting region $j_2/(cE/\xi\Phi_0)$. For $\lambda_2/\lambda_1 = 2$, the transport current density in the strongly superconducting region j_1 is $(\lambda_2/\lambda_1)^2 = 4$ times as large as that in the weakly superconducting region j_2. The vortex is pinned at the positions of the local minima indicated by the solid circles in Fig. 10. As seen in Fig. 10, the pinning position moves toward the interface as the transport current density increases, and reaches the interface at the critical current density $j_2/(cE/\xi\Phi_0) = 6.5$. The total force, which is given by the sum of the driving force Eq. (20) and the pinning forces Eqs. (38) and (41), is plotted in Fig. 11. The total force changes its sign at the pinning positions indicated by the solid circles. The pinning position moves toward the interface as the transport current in-

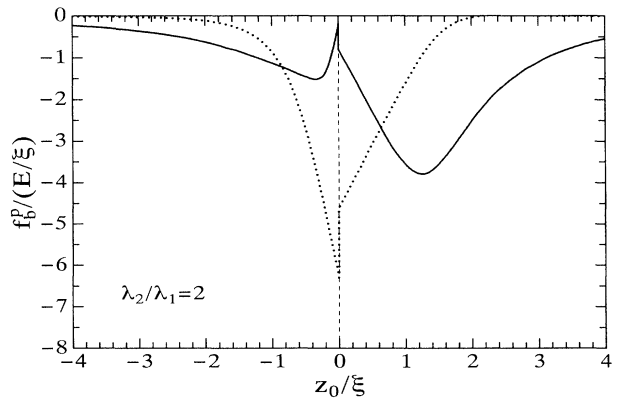

FIG. 8. Electromagnetic pinning force f_b^p is indicated as a function of the vortex center z_0/ξ by the solid curve. The vortex core pinning force is also plotted by the dotted curve.

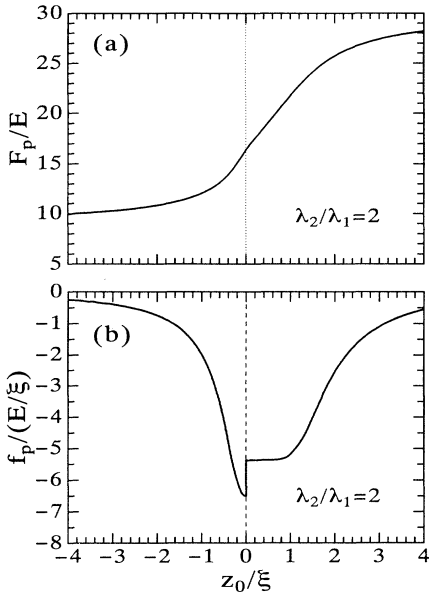

FIG. 9. Total pinning free energy of the vortex F_p and the total pinning force f_p as a function of the vortex center z_0/ξ. (a) The total pinning free energy F_p defined by the sum of the core free energy F_ψ and the electromagnetic free energy F_b^p, and (b) the total pinning force f_p defined by the sum of the core pinning force f_ψ and the electromagnetic pinning force f_b^p.

creases and reaches the interface at the critical current density.

To see the importance of the inhomogeneous distribution of the transport current for the pinning, we consider a fictitious case where the transport current uniformly flows in all regions of the system and its current density is

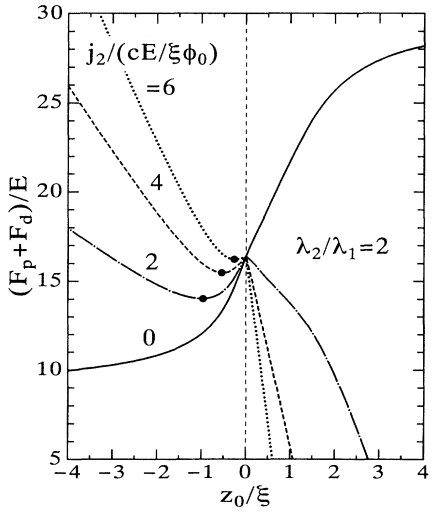

FIG. 10. Sum of the driving free energy F_d and the pinning free energy F_p as a function of the vortex center z_0/ξ. The values of $j_2/(cE/\xi\Phi_0)$ indicate the strength of the driving force acting on the vortex in region 2. The vortex is stabilized at the positions indicated by the solid circles.

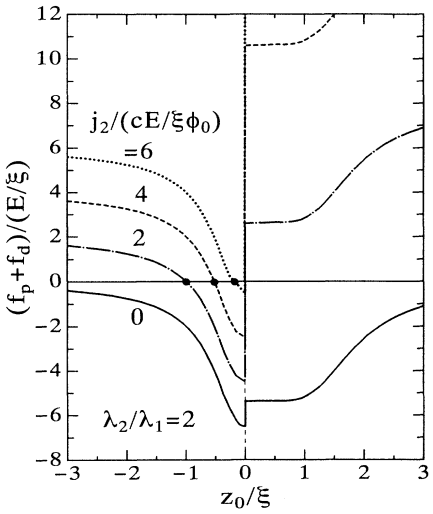

FIG. 11. Sum of the driving force f_d and the pinning force f_p as a function of the vortex center z_0/ξ. The vortex is pinned at the positions indicated by the solid circles where the total force changes its sign.

given by the average of the transport current densities in regions 1 and 2, $(j_1+j_2)/2$. The total free energy in this case is shown in Fig. 12 For the current density $j_2/(cE/\xi\Phi_0)=2$, the vortex is pinned at the local minimum of the free energy appearing near the interface. However, for the current densities of $j_2/(cE/\xi\Phi_0)=4$ and 6, the minimum disappears and thus the vortex is depinned in contrast to the case in Fig. 10. The observed critical current density for the inhomogeneous current distribution is $[1+(\lambda_2/\lambda_1)^2]/2$ times as large as that for the uniform (fictitious) current distribution. The observed critical current density is very much enhanced for a large value of λ_2/λ_1. For the case of $\lambda_2/\lambda_1=2$, the ob-

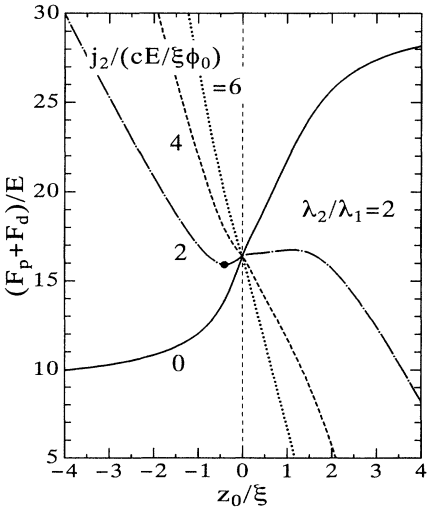

FIG. 12. Fictitious total free energy as a function of the vortex center where we suppose the current density with $(j_1+j_2)/2$ uniformly flows in the system.

served critical current densities for the inhomogeneous and uniform current distributions are 16.25 and 6.5 in units of $cE/\xi\Phi_0$, respectively.

VII. DISCUSSION

As was mentioned in the Introduction, the critical current in $Bi_2Sr_2CaCu_2O_{8+\delta}$ is independent of the relative angle between the directions of the critical current and the applied magnetic field in the film plane.[10,11,39–57] On the other hand, experiments show that in $YBa_2Cu_3O_{7-\delta}$, the critical current in the applied magnetic field parallel to the current is larger than that in the magnetic field perpendicular to the current.[58–60] This difference may be explained within the framework of the present theory in the following way. As shown in Sec. VI, the critical current density due to the pinning for $\lambda_2/\lambda_1=2$ in the magnetic field perpendicular to the current is 16.25 in units of $Ec/\Phi_0\xi$, where E is defined by Eq. (37). The order of magnitude of $Ec/\Phi_0\xi$ for cuprate superconductors is 10^7 A/cm^2. The critical current density increases as the magnetic field deviates from the direction perpendicular to the current. The pair-breaking effect also limits the critical current density. The pair-breaking effect is caused by the kinetic energy of the superconducting current exceeding the superconducting condensation energy.[61,62] The depairing current density due to this effect is estimated to be 11.1 for $\lambda_2/\lambda_1=2$ in the same units of $Ec/\Phi_0\xi$. Since the depairing current density is smaller than the critical current density due to the pinning mentioned above, the observed critical current density is determined by the depairing current density. Therefore, the observed critical current density in this case is independent of the angle between the current and the magnetic field. We suppose that $Bi_2Sr_2CaCu_2O_{8+\delta}$ corresponds to this case.

The calculation shows that the depairing current density increases as λ_2/λ_1 decreases and tends to 17.8 in units of $Ec/\Phi_0\xi$ in the limit of $\lambda_2/\lambda_1=1$. On the other hand, the critical current density due to the pinning drastically decreases as λ_2/λ_1 decreases and vanishes in the limit of $\lambda_2/\lambda_1=1$. Therefore, below a certain value of λ_2/λ_1 the pinning critical current density becomes smaller than the depairing current density. In this case the observed critical current density in the magnetic field perpendicular to the current is determined by the pinning critical current density. The observed critical current density in the magnetic field parallel to the current is still determined by the depairing current density, since there is no driving force in this configuration. As a result, the critical current is anisotropic with respect to the relative angle between the current and the magnetic field. We suppose that this is the case for $YBa_2Cu_3O_{7-\delta}$.

Note added in proof. An extensive survey of superconductivity in layered superconductors is given by a book entitled *Layered Superconductors* by R. A. Klemm (Oxford, New York, 1993).

ACKNOWLEDGMENTS

One of the authors (M.T.) would like to express his sincere thanks to Dr. A. A. Abrikosov for valuable comments and discussions on this work. The authors also thank Dr. T. Koyama, Dr. H. Matsumoto, Dr. X. G. Qiu, and Mr. N. Takezawa for helpful discussions. This work was supported by a Grant-in-Aid for Scientific Research on Priority Area, "Science of High T_c Superconductivity" given by the Ministry of Education, Science and Culture, Japan.

APPENDIX A

In this appendix, we show that $(c/4\pi)\nabla_{\mathbf{r}_0}\times\mathbf{b}_t(\mathbf{r}_0)$ is equal to the *true* transport current $\mathbf{j}_{t0}(\mathbf{r}_0)$, the transport current in the absence of the vortex under consideration. The *microscopic* transport current $\mathbf{j}_t(\mathbf{r})$ and the magnetic field associated with this current $\mathbf{b}_t(\mathbf{r})$ satisfy the Maxwell equation

$$\nabla\times\mathbf{b}_t(\mathbf{r})=\frac{4\pi}{c}\mathbf{j}_t(\mathbf{r}) . \tag{A1}$$

Integrating (A1) with respect to z from $-\infty$ (or ∞) to z_0, we have

$$b_t(0,z_0)=\frac{4\pi}{c}\int_{-\infty}^{z_0} dz\, j_t^y(0,z;z_0) , \tag{A2}$$

where we rewrite $j_t^y(0,z)$ as $j_t^y(0,z;z_0)$, indicating that the microscopic transport current is a functional of z_0. Since Fig. 13(a) shows that the total number of streamlines crossing the part of the z axis between $-\infty$ and z_0 does not depend on whether the vortex is or is not at $(0,z_0)$, $j_t^y(0,z;z_0)$ in Eq. (A2) is replaced by the true transport

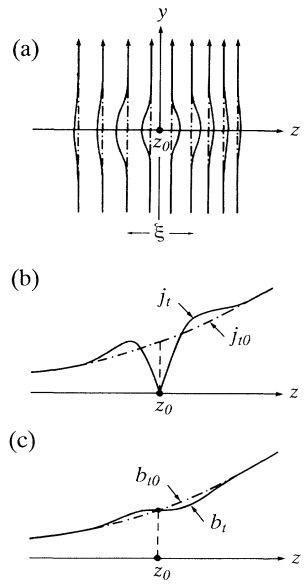

FIG. 13. Schematic representation for the spatial variation of the microscopic and true transport currents, $\mathbf{j}_t(\mathbf{r})$ and $\mathbf{j}_{t0}(\mathbf{r})$, and the magnetic fields induced by these currents, $b_t(\mathbf{r})$ and $b_{t0}(\mathbf{r})$, around the vortex center $(0,z_0)$. (a) The streamlines of the transport currents in the yz plane, (b) the transport current densities as a function of z, and (c) the magnetic fields as a function of z. The solid and dash-dotted curves indicate the currents and magnetic fields with and without the vortex in the system.

current $j_{t0}^{y}(0,z)$ as

$$b_t(0,z_0)=\frac{4\pi}{c}\int_{-\infty}^{z_0} dz\, j_{t0}^{y}(0,z) \ . \tag{A3}$$

Note that $j_{t0}^{y}(0,z)$ is independent of z_0. Taking the derivative of (A3) with respect to z_0, we have

$$\frac{d}{dz_0}b_t(0,z_0)=\frac{4\pi}{c}j_{t0}^{y}(0,z_0) \ , \tag{A4}$$

or

$$\nabla_{\mathbf{r}_0}\times\mathbf{b}_t(\mathbf{r}_0)=\frac{4\pi}{c}\mathbf{j}_{t0}(\mathbf{r}_0) \ . \tag{A5}$$

APPENDIX B

In this appendix, we prove that the average of the true transport current densities at the vortex centers is equal to the observed transport current density. From Eqs. (19) and (A5), the driving force acting on a vortex at $\mathbf{r}_i$ is expressed in terms of the true transport current as

$$\mathbf{f}_d(\mathbf{r}_i)=\frac{\Phi_0}{4\pi}(\nabla_{\mathbf{r}_i}\times\mathbf{b}_t(\mathbf{r}_i))\times\mathbf{e}_x=\frac{\Phi_0}{c}\mathbf{j}_{t0}(\mathbf{r}_i)\times\mathbf{e}_x \ . \tag{B1}$$

The driving force acting on the vortices intersecting a unit area Γ in the yz plane is given by

$$\mathbf{F}_d=\sum_{i\in\Gamma}\mathbf{f}_d(\mathbf{r}_i)=\frac{\Phi_0}{c}\sum_{i\in\Gamma}\mathbf{j}_{t0}(\mathbf{r}_i)\times\mathbf{e}_x \ . \tag{B2}$$

It is shown from the thermodynamic argument[63–66] that the observed transport current density $\mathbf{J}_T$ is given by

$$\mathbf{F}_d=\frac{n\Phi_0}{c}\mathbf{J}_T\times\mathbf{e}_x \ , \tag{B3}$$

where n is the number of vortices in the area Γ. From Eqs. (B2) and (B3), we have

$$\mathbf{J}_T=\frac{1}{n}\sum_{i\in\Gamma}\mathbf{j}_{t0}(\mathbf{r}_i) \ . \tag{B4}$$

Thus the observed transport current density is given by the average of the true transport current densities at the vortex centers.

APPENDIX C

For the purpose of obtaining the boundary condition Eq. (21), we insert a fictitious intermediate region I between regions 1 and 2. In region I, the penetration depth changes as it connects smoothly with the penetration depths in regions 1 and 2, as shown in Fig. 14. The free energy of region I is given by

$$F_b^{t0}=\int_{\mathrm{I}}d\mathbf{r}\left[\frac{2\pi}{c^2}\lambda_{\mathrm{I}}^2(z)\mathbf{j}_{t0}^2(\mathbf{r})+\frac{1}{8\pi}\mathbf{b}_{t0}^2(\mathbf{r})\right] \ , \tag{C1}$$

where $\mathbf{b}_{t0}(\mathbf{r})$ is the magnetic field induced by the true transport current $\mathbf{j}_{t0}(\mathbf{r})$, and $\lambda_{\mathrm{I}}(z)$ is the penetration depth in region I. By using the Maxwell equation and integrating the free energy Eq. (C1) by parts, the free energy is rewritten as

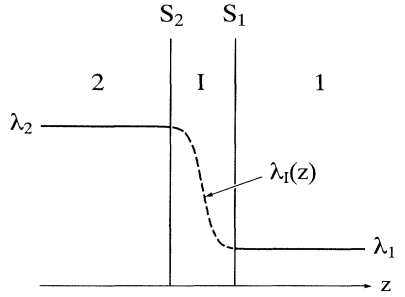

FIG. 14. Junction consisting of the superconductors 1, I, and 2. The penetration depth $\lambda_{\mathrm{I}}(z)$ indicated by the dashed curve smoothly changes in region I, and connects with λ_1 at the interface S_1 and with λ_2 at the interface S_2. In the limit of region I vanishing, the junction changes to the interface shown in Fig. 1.

$$F_b^{t0}=-\int_{S_1}dS\frac{\lambda_{\mathrm{I}}^2(z)}{2c}[\mathbf{b}_{t0}(\mathbf{r})\times\mathbf{j}_{t0}(\mathbf{r})]_{\mathrm{I}}\cdot\mathbf{e}_z +\int_{S_2}dS\frac{\lambda_{\mathrm{I}}^2(z)}{2c}[\mathbf{b}_{t0}(\mathbf{r})\times\mathbf{j}_{t0}(\mathbf{r})]_{\mathrm{I}}\cdot\mathbf{e}_z \ , \tag{C2}$$

where dS is the surface element in the interfaces and $\mathbf{e}_z$ is the unit vector in the direction of the z axis. In Eq. (C2), S_1 and S_2 denote the surfaces of region I, which contact with regions 1 and 2, respectively, and the subscript I denotes region I. Since $\mathbf{j}_{t0}(\mathbf{r})$ and $\mathbf{b}_{t0}(\mathbf{r})$ are continuous at the interfaces, the free energy Eq. (C2) is written as

$$F_b^{t0}=-\frac{\lambda_1^2}{2c}\int_{S_1}dS[\mathbf{b}_{t0}(\mathbf{r})\times\mathbf{j}_{t0}(\mathbf{r})]_1\cdot\mathbf{e}_z +\frac{\lambda_2^2}{2c}\int_{S_2}dS[\mathbf{b}_{t0}(\mathbf{r})\times\mathbf{j}_{t0}(\mathbf{r})]_2\cdot\mathbf{e}_z \ , \tag{C3}$$

the subscripts 1 and 2 indicating regions 1 and 2, respectively. If we take a limit of the separation between S_1 and S_2 vanishing, the free energy in Eq. (C1) vanishes, because of the integrand in Eq. (C1) having finite values. Thus, in the same limit, the free energy Eq. (C3) vanishes. Then, if we used the condition that $b_{t0}(\mathbf{r})$ is continuous at the interface, from Eq. (C3) we have the boundary condition Eq. (21).

APPENDIX D

A square domain of $-L\le y,z\le L$ in the yz plane is divided into $2N\times 2N$ meshes. The y and z variables are discretized with an equal step $d=L/N$ to the mesh points (y_l,z_l). The amplitude of the order parameter and the vector potential at the mesh point (y_l,z_l) are denoted by ψ_l and $\mathbf{A}_l$, respectively. Using the difference formulas to evaluate the derivatives, we transform the differential equations (25) and (26) into the difference equations for ψ_l and $\mathbf{A}_l$. Starting from an initial guess for $\psi_l^{(1)}$ and $\mathbf{A}_l^{(1)}$, we iterate the order parameter and the vector potential by the relaxation method[67,68]

$$\psi_l^{(n+1)}=\psi_l^{(n)}+\eta G_l^{\psi} \ , \tag{D1}$$

$$\mathbf{A}_l^{(n+1)} = \mathbf{A}_l^{(n)} + \eta \mathbf{G}_l^{\mathbf{A}} , \tag{D2}$$

where G_l^{ψ} and $\mathbf{G}_l^{\mathbf{A}}$ are, respectively, the difference representation for the left-hand sides of Eqs. (25) and (26), that is, $G_l^{\psi}=0$ and $\mathbf{G}_l^{\mathbf{A}}=\mathbf{0}$, are, respectively, the difference equations for Eqs. (25) and (26), and η is a converging parameter ($\eta < \frac{1}{4}$). In the calculation, we used $d/\xi=0.1$, $\eta=0.2$, and $N=100$. The dimension of the domain is $20\xi \times 20\xi$. Outside the domain, we fixed $\psi_l=\psi_1$ for $z \geq 0$ and $\psi_l=\psi_2$ for $z \leq 0$, and used the London solution for $\mathbf{A}_l$. The self-consistency for $\psi_l^{(n)}$ and $\mathbf{A}_l^{(n)}$ is taken under boundary conditions Eqs. (28), (32), (33), and (34) at the interface. We break off the iteration when the converging conditions $G_l^{\psi}/\psi_1 < 10^{-5}$ and $\mathbf{G}_l^{\mathbf{A}}/(\Phi_0/2\pi\lambda_1^3) < 10^{-5}$ are fulfilled.

[1]B. Roas, L. Schultz, and G. Saemann-Ischenko, Phys. Rev. Lett. **64**, 479 (1990).

[2]S. Awaji, K. Watanabe, N. Kobayashi, H. Yamane, and H. Hirai, Jpn. J. Appl. Phys. **31**, L1532 (1992).

[3]C. Tomé-Rosa, G. Jakob, A. Walkenhorst, M. Maul, M. Schmitt, M. Paulson, and H. Adrian, Z. Phys. B **83**, 221 (1991).

[4]J. W. Ekin, Appl. Phys. Lett. **59**, 360 (1991).

[5]R. M. Schalk, H. W. Weber, Z. H. Barder, C. E. Davies, J. E. Evetts, R. E. Somekh, and D. H. Kim, Supercond. Sci. Technol. **5**, S224 (1992).

[6]B. D. Biggs, M. N. Kunchur, J. J. Lin, S. J. Poon, T. R. Askew, R. B. Flippen, M. A. Subramanian, J. Gopalakrishnan, and A. W. Sleight, Phys. Rev. B **39**, 7309 (1989).

[7]H. Raffy, S. Labdi, O. Laborde, and P. Monceau, Physica B **165-166**, 1423 (1990).

[8]P. Schmitt, P. Kummeth, L. Schultz, and G. Saemann-Ischenko, Phys. Rev. Lett. **67**, 267 (1991).

[9]H. Yamasaki, K. Endo, S. Kosaka, M. Umeda, S. Misawa, S. Yoshida, and K. Kajimura, IEEE Trans. Supercond. (to be published); H. Yamasaki, K. Endo, Y. Nakagawa, M. Umeda, S. Kosaka, S. Misawa, S. Yoshida, and K. Kajimura, J. Appl. Phys. **72**, 2951 (1992).

[10]Y. Iye, S. Nakamura, and T. Tamegai, Physica C **159**, 433 (1989).

[11]Y. Horie, K. Miyosi, D. H. Lee, T. Nisizaki, F. Ichikawa, T. Fukami, and T. Aomine (unpublished).

[12]M. Tachiki and S. Takahashi, Solid State Commun. **70**, 291 (1989); **72**, 1083 (1989); M. Tachiki and S. Takahashi, Physica B **169**, 121 (1990); T. Koyama, N. Takezawa, and M. Tachiki, Physica C **172**, 501 (1991); M. Tachiki, T. Koyama, and S. Takahahi, *ibid.* **185-189**, 303 (1991).

[13]J. Friedel, J. Phys.: Condens. Matter **1**, 7757 (1989).

[14]B. I. Ivlev and N. B. Kopnin, Phys. Rev. Lett. **64**, 1828 (1990).

[15]D. Feinberg and C. Villard, Phys. Rev. Lett. **65**, 919 (1990).

[16]S. Chakravatry, B. I. Ivlev, and Y. N. Ovchinnikov, Phys. Rev. B **42**, 2143 (1990); Phys. Rev. Lett. **64**, 3187 (1990).

[17]C. Dasgupta and T. V. Ramakrishnan, in *Proceedings of the International Conference on Superconductivity,* edited by S. K. Joshi *et al.* (World Scientific, Singapore, 1991), p. 432.

[18]V. G. Kogan and J. L. Campbell, Phys. Rev. Lett. **62**, 1552 (1989).

[19]Y. Iye, T. Terashima, and Y. Bando, Physica C **177**, 393 (1991); **184**, 362 (1992); Y. Iye, A. Fukushima, T. Tamegai, T. Terashima, and Y. Bando, *ibid.* **185-189**, 297 (1991).

[20]W. K. Kwok, U. Welp, V. M. Vinokur, S. Fleshler, J. Downey, and G. W. Crabtree, Phys. Rev. Lett. **67**, 390 (1991).

[21]K. E. Gray and D. H. Kim, Physica C **180**, 139 (1991).

[22]D. K. Christen, C. E. Klabunde, J. R. Thompson, H. R. Kerchner, S. T. Sekula, R. Feenstra, and J. D. Dudai, Physica C **162-164**, 653 (1989).

[23]Y. Kuwasawa, T. Yamaguchi, T. Tosaka, S. Aoki, S. Nakano, and S. Matsuda, Physica C **169**, 39 (1990).

[24]T. Nisizaki, T. Aomine, I. Fujii, K. Yamamoto, S. Yoshii, T. Terashima, and Y. Bando, Physica C **181**, 223 (1991); T. Fukami, K. Hayashi, T. Yamamoto, T. Nisizaki, Y. Horie, F. Ichikawa, T. Aomine, V. Soares, and L. Rinderer, *ibid.* **184**, 65 (1991).

[25]A. J. Vermeer, D. G. de Groot, N. J. Koeman, R. Griessen, and C. van Hæsendonck, Physica C **185-189**, 2345 (1991).

[26]B. Y. Jin and J. B. Ketterson, Adv. Phys. **38**, 189 (1989).

[27]V. Matijasevic and M. R. Beasley, *Metallic Superlattices,* edited by T. Shinjo and T. Takada (Elsevier, Amsterdam, 1987), p. 187.

[28]P. R. Broussard and T. H. Geballe, Phys. Rev. B **37**, 68 (1988); J. L. Cohn, J. J. Lin, F. J. Lamelas, H. He, R. Clarke, and C. Uher, *ibid.* **38**, 2326 (1988).

[29]J-M. Triscone, Ø. Fischer, O. Brunner, L. Antognazza, A. D. Kent, and M. G. Karkut, Phys. Rev. Lett. **64**, 804 (1990).

[30]Q. Li, X. X. Xi, X. D. Wu, A. Inam, S. Vadlamannati, W. L. McLean, T. Venkatesan, R. Ramesh, D. M. Hwang, J. A. Martinez, and L. Nazar, Phys. Rev. Lett. **64**, 3086 (1990).

[31]D. Lowndes, D. P. Norton, and J. D. Budai, Phys. Rev. Lett. **65**, 1160 (1990).

[32]T. Terashima, K. Shimura, Y. Bando, Y. Matusda, A. Fujiyama, and S. Komiyama, Phys. Rev. Lett. **67**, 1362 (1991).

[33]G. Jakob, P. Przyslupski, C. Stolzel, C. Tomé-Rosa, A. Walkenhorst, M. Schmitt, and H. Adrian, Appl. Phys. Lett. **59**, 1626 (1991).

[34]E. E. Fullerton, J. Guimpel, O. Nakamura, and I. K. Schuller, Phys. Rev. Lett. **69**, 2859 (1992).

[35]C.-B. Eom, J.-M. Triscone, Y. Suzuki, and T. H. Geballe, Physica C **185-189**, 2065 (1991).

[36]A. A. Abrikosov, *Fundamentals of the Theory of Metals* (North-Holland, Amsterdam, 1988).

[37]P. G. de Gennes, *Superconductivity of Metals and Alloys* (Benjamin, New York, 1966), p. 235.

[38]R. O. Zaitsev, Zh. Eksp. Teor. Fiz. **50**, 1055 (1966) [Sov. Phys. JETP **23**, 702 (1966)].

[39]K. Kitazawa, S. Kambe, M. Naito, I. Tanaka, and H. Kojima, Jpn. J. Appl. Phys. **28**, L555 (1989).

[40]K. Kadowaki, in *Proceedings of the International Workshop on Electronic Properties and Mechanisms in High-T_c Superconductors,* edited by T. Oguchi, K. Kadowaki, and T. Sasaki (North-Holland, Amsterdam, 1992), p. 209.

[41]Y. Ando. N. Motohira, K. Kitazawa, J. Takeya, and S. Akita, Phys. Rev. Lett. **67**, 2737 (1991).

[42]D. E. Farrell, S. Bonham, J. Foster, Y. C. Chang, P. Z. Jiang, K. G. Vandervoort, D. J. Lam, and V. G. Kogan, Phys. Rev. Lett. **63**, 782 (1989).

[43]M. Tuominen, A. M. Goldman, Y. C. Chang, and P. Z. Jiang, Phys. Rev. B **42**, 8740 (1990).

[44]R. Hergt, W. Andrä, and K. Fischer, Physica C **185-189**, 2197 (1991).

[45]R. Flutcher, C. Aguillon, I. A. Campbell, and B. Keszei, Phys. Rev. B **42**, 2627 (1990).
[46]K. Okuda, S. Kawamata, S. Noguchi, N. Itoh, and K. Kadowaki, J. Phys. Soc. Jpn. **60**, 3226 (1991).
[47]K. C. Woo, K. E. Gray, R. T. Kampwirth, J. H. Kang, S. J. Stein, R. East, and D. M. McKay, Phys. Rev. Lett. **63**, 1877 (1989); D. H. Kim, K. E. Gray, R. T. Kampwirth, and D. M. McKay, Phys. Rev. B **42**, 6249 (1990).
[48]R. C. Budhani, D. O. Welch, M. Suenaga, and R. L. Sabatini, Phys. Rev. Lett. **64**, 1666 (1990).
[49]W. Maj, K.-J. de Korver, P. Koorevaar, and J. Aarts, Supercond. Sci. Technol. **5**, S483 (1992); T. Nojima, M. Kinosita, Y. Kuwasawa, and S. Nakano (unpublished).
[50]P. H. Kes, J. Aarts, V. M. Vinokur, and C. J. van der Beek, Phys. Rev. Lett. **64**, 1063 (1990).
[51]S. Doniach, in *High-Temperature Superconductivity,* edited by K. S. Bedell *et al.* (Addison-Wesley, Reading, MA, 1990), p. 406.
[52]J. R. Clem, Phys. Rev. B **43**, 7837 (1991).
[53]L. N. Bulaevksii, Phys. Rev. B **44**, 910 (1991).
[54]V. M. Vinokur, P. H. Kes, and A. E. Koshelev, Physica C **168**, 29 (1990).
[55]M. V. Feigel'man, V. B. Geshkenbein, and A. I. Larkin, Physica C **167**, 177 (1990).
[56]E. H. Brandt, Physica C **195**, 1 (1992).
[57]G. Blatter, B. I. Ivlev, and J. Rhyner, Phys. Rev. Lett. **66**, 2392 (1991).
[58]W. K. Kwok, U. Welp, G. W. Crabtree, K. G. Vandervoort, R. Hulscher, and J. Z. Liu, Phys. Rev. Lett. **64**, 966 (1990).
[59]J. N. Li, Z. Tarnawski, and J. J. M. Franse, Physica C **180**, 411 (1991).
[60]K. Watanabe, H. Yamane, N. Kobayashi, H. Hirai, and Y. Muto, in *Studies of High-Temperature Superconductors,* edited by A. V. Narlikar (Nova Science, New York, 1991), Vol. 8, p. 132.
[61]M. Tinkham, *Introduction to Superconductivity* (McGraw-Hill, New York, 1975), p. 118.
[62]J. Mannhart, in *Earlier and Recent Aspects of Superconductivity,* edited by J. G. Bednorz and K. A. Müller (Springer-Verlag, Berlin, 1990), p. 208; P. Chaudhari, D. Dimos, and J. Mannhart, *ibid.*, p. 201.
[63]J. Friedel, P. G. de Gennes, and J. Matricon, Appl. Phys. Lett. **2**, 199 (1963).
[64]B. D. Josephson, Phys. Rev. **152**, 211 (1966).
[65]A. M. Campbell and J. E. Evetts, Adv. Phys. **21**, 199 (1972).
[66]H. Ullmaier, *Irreversible Properties of Type-II Superconductors* (Springer-Verlag, Berlin, 1975), p. 145.
[67]E. V. Thuneberg, Phys. Rev. B **36**, 3583 (1987).
[68]T. A. Tokuyasu, D. W. Hess, and J. A. Sauls, Phys. Rev. B **41**, 8891 (1990).